

Complexation of trivalent lanthanide cations by galactitol in the solid state. The crystal structure and an FT-IR study of $2\text{NdCl}_3 \cdot \text{galactitol} \cdot 14\text{H}_2\text{O}$

Limin Yang, Ying Zhao, Wen Tian, Xianglin Jin, Shifu Weng, Jinguang Wu*

College of Chemistry and Molecular Engineering, Peking University–The University of Hong Kong Joint Laboratory in Rare Earth Materials and Bioinorganic Chemistry, Peking University, Beijing 100871, PR China

Received 9 February 2000; accepted 25 September 2000

Abstract

The crystal structure of $2\text{NdCl}_3 \cdot \text{galactitol} \cdot 14\text{H}_2\text{O}$ has been determined. The crystal system is triclinic, space group: -1 , with unit-cell dimensions: $a = 9.736(2)$, $b = 10.396$, $c = 8.027$ Å; $\alpha = 108.05(3)$, $\beta = 92.68(3)$, $\gamma = 88.44(3)^\circ$, $V = 771.6(3)$ Å³, $Z = 2$. Each Nd atom is coordinated to nine oxygen atoms, three from the alditol and six from water molecules, with Nd–O distances from 2.461 to 2.552 Å. The seventh water molecule is hydrogen-bonded by the hydroxyl hydrogen on O-1 (O-1–H-11...O-10, 2.639 Å). The FT-IR spectra of $2\text{NdCl}_3 \cdot \text{galactitol} \cdot 14\text{H}_2\text{O}$ and $2\text{PrCl}_3 \cdot \text{galactitol} \cdot 14\text{H}_2\text{O}$ are analogous, and show that Pr and Nd have the same coordination mode. The IR results are consistent with the crystal structures. © 2001 Elsevier Science Ltd. All rights reserved.

Keywords: Lanthanide; Alditol; Crystal structure; FT-IR

1. Introduction

The metal-binding properties of carbohydrates have been shown to be of fundamental importance in many biochemical processes, such as the transport and storage of metals,^{1,2} the mechanism of action of metal-containing pharmaceuticals, toxic-metal metabolism,^{3,4} and Ca(II)-mediated carbohydrate–protein binding.^{5,6} A series of reviews on the interaction between metals and sugars has been published.^{7–18} Although coordination chemistry plays a central role in these processes, relatively few well-characterized complexes of

metals with carbohydrate ligands have been reported.^{19,20}

Lanthanide complexes are often used as shift reagents to probe metal-binding sites in aqueous solution. As biologically non-necessary elements, rare earth ions have novel biological effects of medical significance.²¹ Rare earth compounds are also used in agricultural fertilizers or as feed additives in animal husbandry.²² Some attention has been paid to the biological effect of rare earth ions.^{23–25} Interactions take place between lanthanide ions and carbohydrates. TLC results show that alditols form stronger complexes with Pr^{3+} , Nd^{3+} , Sm^{3+} , and Eu^{3+} than with La^{3+} , and Ca^{2+} .^{26,27} Galactitol is found, for example, in seaweed and is the sole constituent of Madagascar Manna.²⁸ It occurs in the cataractous lenses of galactosemic animals as a metabolic

* Corresponding author. Fax: +86-10-62751708.

E-mail address: wjg@chemms.chem.pku.edu.cn (J. Wu).

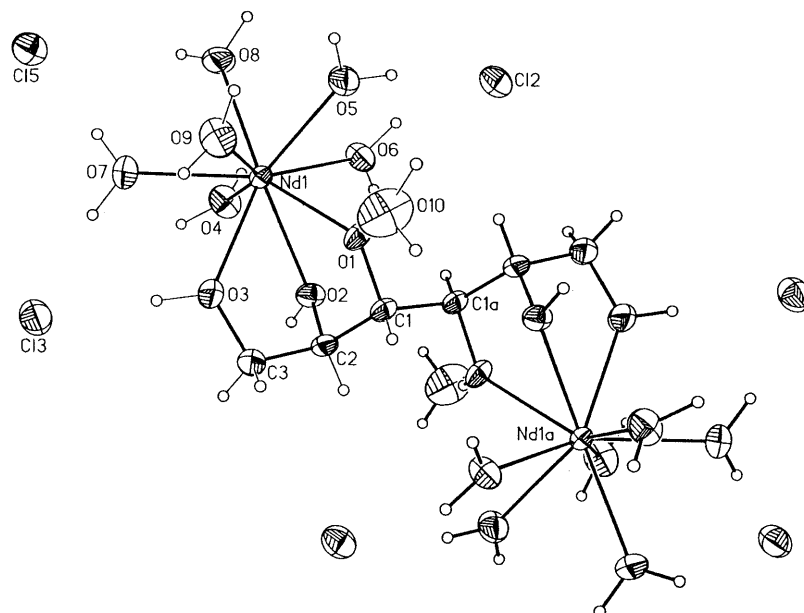


Fig. 1. The structure and atom numbering scheme of $2\text{NdCl}_3 \cdot \text{galactitol} \cdot 14\text{H}_2\text{O}$.

product of galactose, causing a hypertonic condition whereby water is drawn into the lens fibres, which become opaque and may eventually rupture.²⁹

The crystal structure of $2\text{PrCl}_3 \cdot \text{galactitol} \cdot 14\text{H}_2\text{O}$ has been reported and is the first crystal structure of an alditol–lanthanide complex.²⁷ Galactitol was therefore chosen as a model to study the interaction between lanthanide ions and sugars. It is necessary to study the coordination regularity of lanthanide ions, because lanthanide ions with various f-electronic configurations have different coordination modes, as in the coordination of lanthanide ions to 4-aminobenzenesulfonic acid.³⁰ The synthesis and isolation of crystalline metal–sugar complexes are difficult and it is not easy to obtain crystal structures of the complexes. IR is also an important technique for studying the formation of metal–sugar complexes.^{31–35} The IR technique is therefore used to study the coordination regularity of lanthanide ions and to assign unknown coordinate structures from similarities of IR spectra. This paper reports the crystal structure of $2\text{NdCl}_3 \cdot \text{galactitol} \cdot 14\text{H}_2\text{O}$. The FT-IR spectra of $2\text{NdCl}_3 \cdot \text{galactitol} \cdot 14\text{H}_2\text{O}$ and $2\text{PrCl}_3 \cdot \text{galactitol} \cdot 14\text{H}_2\text{O}$ are in excellent agreement with the results of crystal structures, and provide a basis for the study of coordination regularity of lanthanide ions with sugars.

2. Results and discussion

The structure and atom-numbering scheme is shown in Figs. 1 and 2 is a projection of the crystal cell in the crystal structure of $2\text{NdCl}_3 \cdot \text{galactitol} \cdot 14\text{H}_2\text{O}$. Crystal data are listed in Table 1. The crystal structure of $2\text{NdCl}_3 \cdot \text{galactitol} \cdot 14\text{H}_2\text{O}$ is analogous with the corresponding Pr-complex.²⁷ The numbering is not by carbohydrate conventions, but crys-

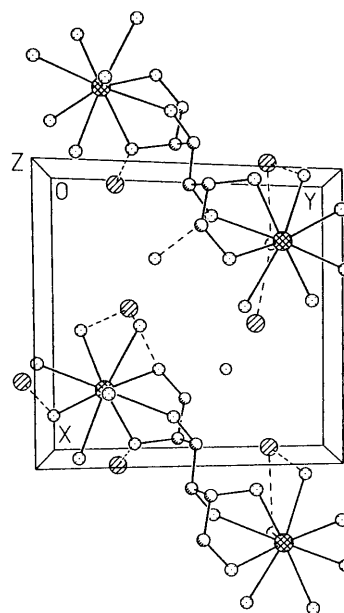


Fig. 2. The projection of the crystal cell in the crystal structure of $2\text{NdCl}_3 \cdot \text{galactitol} \cdot 14\text{H}_2\text{O}$.

Table 1

Crystal data and structure refinement of 2NdCl₃·galactitol·14H₂O

Empirical formula	C ₃ H ₂₁ Cl ₃ NdO ₁₀
Formula weight	467.79
Temperature (K)	293(2)
Wavelength (Å)	0.71073
Crystal system, space group	triclinic, $P\bar{1}$
Unit cell dimensions	
<i>a</i> (Å)	9.736(2)
<i>b</i> (Å)	10.396(2)
<i>c</i> (Å)	8.027(2)
α (°)	108.05(3)
β (°)	$\beta = 92.68(3)$
γ (°)	88.44(3)
<i>V</i> (Å ³)	71.6(3)
<i>Z</i> , <i>D</i> _{calcd} (g cm ⁻³)	2, 2.014
Absorption coefficient (mm ⁻¹)	3.916
<i>F</i> (000)	460
Crystal size (mm)	0.40 × 0.35 × 0.30
Theta range for data collection (°)	2.06–25.00
Index ranges	$0 \leq h \leq 11$, $-12 \leq k \leq 12$, $-9 \leq l \leq 9$
Reflections collected/unique	2908/2731 [<i>R</i> _{int} = 0.0210]
Completeness to $2\theta = 25.00$	99.9%
Absorption correction	Psi scan
Max. and min. transmission	1.0000 and 0.7685
Refinement method	Full-matrix least-squares on <i>F</i> ²
Data/restraints/parameters	2731/17/223
Goodness-of-fit on <i>F</i> ²	0.968
Final <i>R</i> indices [<i>I</i> > 2σ(<i>I</i>)]	<i>R</i> ₁ = 0.0228, <i>wR</i> ₂ = 0.0598
<i>R</i> indices (all data)	<i>R</i> ₁ = 0.0240, <i>wR</i> ₂ = 0.0605
Extinction coefficient	0.0142(9)
Largest difference peak and hole (e Å ⁻³)	0.877 and -1.146

tallographic: the unit being centrosymmetrical, the same numbers were allocated to corresponding atoms in the two asymmetric half-units (Fig. 1). Atomic parameters are given in Table 2. Selected bond lengths and bond angles are shown in Table 3.

Each Nd atom is coordinated to nine oxygen atoms, three from the alditol and six from water molecules, with Nd–O distances from 2.461 to 2.552 Å. The seventh water molecule is hydrogen-bonded by the hydroxyl hydrogen on O-1 (O-1–H-11···O-10, 2.639 Å). Galactitol has the threo configuration between O-2, O-3 and O-4, O-5, and therefore, it should form a substantial proportion of a 1:2 complex. No

direct contact exists between Nd³⁺ and Cl⁻ (Nd–Cl-2, 4.05 Å; Nd–Cl-3, 4.77 Å; Nd–Cl-5, 4.93 Å). As would be expected, there is an extensive network of hydrogen bonds involving hydroxyl groups, water molecules, and chloride ions. The minimum Cl–O distance is Cl-3–O-7, 2.81 Å.

The C–O, C–C bond distances and the bond angles of galactitol, Pr-galactitol, and Nd-galactitol are listed in Table 4.^{27,36} The molecular symmetry of galactitol is approximately -1 and the others: -1 space group. In comparison with the galactitol structure, the C-1–O-1, and C-2–O-2 distances are longer in the metal–complex structures and C-3–O-3 is longer in the Nd-complex and shorter in the Pr-complex. The C-1–C-2 distances are shorter and C-2–C-3, C-1–C-1# are longer in the crystal structure of the complexes. The angles (O-3–C-3–C-2, C-3–C-2–O-2, O-2–C-2–C-1, C-2–C-1–O-1, O-1–C-1–C-1#, C-2–C-1–C-1#) are smaller and C-1–C-2–C-3 is larger in the complex structures. Although the Pr- and Nd-complexes have the same coordination mode (the same coordination number and chelated sites), there are some differences in the bond distances and angles between the two crystal structures. The characteristic colors of the complexes are light green and purple, respectively.

Table 2

Atomic coordinates ($\times 10^4$) and *U*_{eq}

	<i>x</i>	<i>y</i>	<i>z</i>	<i>U</i> _{eq} ^a
Nd-1	2519(1)	7897(1)	1430(1)	20(1)
Cl-2	-376(1)	7628(1)	-3585(1)	37(1)
Cl-3	5242(1)	7191(1)	6280(1)	42(1)
Cl-5	7388(1)	9069(1)	2203(2)	44(1)
O-1	1673(3)	5640(3)	-287(3)	26(1)
O-2	607(3)	6958(3)	2718(3)	26(1)
O-3	3171(3)	6137(3)	2958(4)	43(1)
O-4	1561(3)	9660(3)	3929(4)	38(1)
O-5	2503(3)	7662(3)	-1738(4)	37(1)
O-6	290(3)	8686(3)	491(4)	34(1)
O-7	4476(3)	8734(3)	3553(4)	36(1)
O-8	3408(4)	9990(3)	1076(4)	44(1)
O-9	4667(3)	6701(4)	55(4)	44(1)
O-10	3066(5)	3773(4)	-2624(6)	65(1)
C-1	715(4)	4922(3)	401(5)	22(1)
C-2	799(4)	5519(4)	2374(5)	24(1)
C-3	2148(4)	5265(4)	3246(6)	34(1)

^a *U*_{eq} is defined as one third of the trace of the orthogonalized *U*_{*ij*} tensor.

Table 3

Bond lengths (Å) and angles (°)^a

Bond length (Å)			
Nd-1-O-4	2.461(3)	Nd-1-O-3	2.552
Nd-1-O-8	2.463(3)	O-1-C-1	1.440(4)
Nd-1-O-1	2.465(3)	O-2-C-2	1.443(4)
Nd-1-O-6	2.467(3)	O-3-C-3	1.438(5)
Nd-1-O-5	2.477(3)	C-1-C-2	1.510(5)
Nd-1-O-7	2.482(3)	C-1-C-1a # 1	1.533(7)
Nd-1-O-9	2.522(3)	C-2-C-3	1.515(6)
Nd-1-O-2	2.528(3)		
Bond angles (°)			
O-4-Nd-1-O-8	77.49(11)	O-1-Nd-1-O-2	63.36(8)
O-4-Nd-1-O-1	131.47(10)	O-6-Nd-1-O-2	71.04(9)
O-8-Nd-1-O-1	141.65(10)	O-5-Nd-1-O-2	121.37(9)
O-4-Nd-1-O-6	70.98(10)	O-7-Nd-1-O-2	112.84(10)
O-8-Nd-1-O-6	84.40(11)	O-9-Nd-1-O-2	128.24(10)
O-1-Nd-1-O-6	83.82(10)	O-4-Nd-1-O-3	98.90(11)
O-4-Nd-1-O-5	131.52(11)	O-8-Nd-1-O-3	139.98(10)
O-8-Nd-1-O-5	71.22(11)	O-1-Nd-1-O-3	68.75(10)
O-1-Nd-1-O-5	70.45(10)	O-6-Nd-1-O-3	132.75(10)
O-6-Nd-1-O-5	69.96(10)	O-5-Nd-1-O-3	128.77(11)
O-4-Nd-1-O-7	73.89(11)	O-7-Nd-1-O-3	70.60(10)
O-8-Nd-1-O-7	70.16(11)	O-9-Nd-1-O-3	73.00(11)
O-1-Nd-1-O-7	134.67(10)	O-2-Nd-1-O-3	62.47(9)
O-6-Nd-1-O-7	140.21(10)	C-1-O-1-Nd-1	121.9(2)
O-5-Nd-1-O-7	125.23(10)	C-2-O-2-Nd-1	110.2(2)
O-4-Nd-1-O-9	146.12(11)	C-3-O-3-Nd-1	120.6(2)
O-8-Nd-1-O-9	87.98(13)	O-1-C-1-C-2	107.3(3)
O-1-Nd-1-O-9	77.28(10)	O-1-C-1-C-1a # 1	107.9(4)
O-6-Nd-1-O-9	138.44(10)	C-2-C-1-C-1a # 1	113.0(4)
O-5-Nd-1-O-9	68.90(11)	O-2-C-2-C-1	105.3(3)
O-7-Nd-1-O-9	72.40(11)	O-2-C-2-C-3	108.8(3)
O-4-Nd-1-O-2	69.35(10)	C-1-C-2-C-3	115.0(3)
O-8-Nd-1-O-2	143.54(11)	O-3-C-3-C-2	108.7(3)

^a Symmetry transformations used to generate equivalent atoms: # 1 $-x, -y+1, -z$.

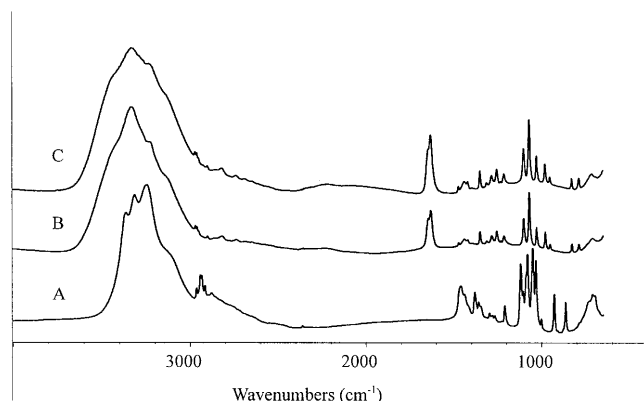


Fig. 3. The mid-IR spectra of galactitol, Pr-galactitol and Nd-galactitol. (A) Galactitol; (B) Pr-galactitol; (C) Nd-galactitol.

The FT-IR spectra are shown in Fig. 3. The results of the spectral analysis are described next.

In the 4000–3000 cm^{-1} region, the stretching-vibration peaks of the OH groups in the spectra of the Pr- and Nd-complexes are broadened in comparison with the spectrum of the free alditol. This broad peak could be assigned to OH stretching vibrations of the alditol, and the water OH stretching vibration is influenced by the extensive hydrogen-bonding network. When the complexes form, the peak positions of free galactitol in this region (3363, 3313, 3243 cm^{-1}) undergo change (3332, 3323, 3239 cm^{-1} for the Pr-complex; 3347, 3332, 3321, 3233 cm^{-1} for the Nd-complex) and the peaks are broadened. The width at half-highest of the peak in the Nd-complex spectrum is greater than that in the spectrum of the Pr-complex, and this is caused by OH coordination. The interaction between metal ion and oxygen broadens the OH stretching vibration peak and the extent of broadening is related to the M–O distance.

When the metal complexes are formed, the relative intensities of the CH stretching vibrations are clearly decreased and peak positions are shifted in the spectra of the metal complexes in the 3000–2000 cm^{-1} region. The peak positions are as follows: 2964, 2943, 2935, 2916, 2897, 2879 cm^{-1} for galactitol, 2971, 2961, 2953, 2901, 2858, 2819 cm^{-1} for Pr-galactitol, and 2972, 2962, 2953, 2902, 2853, 2820 cm^{-1} for Nd-galactitol. The 2820 cm^{-1} peak is the symmetric CH_2 stretching vibration. The formation of M–O bands results in a change of the CH stretching vibrations. The OH vibrations mask the CH bands.

The presence of a broad absorption band at $\sim 3200 \text{ cm}^{-1}$ (related to the OH stretching vibration of water) and medium bands at $\sim 1640 \text{ cm}^{-1}$ (due to the water bending-mode), which are absent from the spectrum of the free alditol, are assigned to the bonded H_2O molecules. In particular, the peak at $\sim 1640 \text{ cm}^{-1}$ splits into two (1642 and 1629 cm^{-1}). The curvefit result for Nd-galactitol is shown in Fig. 4. The two peaks could be split into more peaks, corresponding to various water molecules in the structure. The relative intensities of the two peaks to the 1067 cm^{-1} peak

in the spectra of Pr-galactitol and Nd-galactitol are different. The relative intensities of the two peaks to that at 1067 cm^{-1} in the spectrum of Nd-galactitol are stronger than those in corresponding Pr-galactitol spectrum, maybe because the Nd–O length is shorter than Pr–O and the influence of Nd on water molecules is stronger than Pr.

Within the $1500\text{--}650\text{ cm}^{-1}$ region, for the sugar itself, the ranges include $1500\text{--}1200\text{ cm}^{-1}$, which may be called the local symmetry region, because it is mainly constituted of the deformational vibrations of groups having a local symmetry, such as HCH, and the vibrations of the CH_2OH group; $1200\text{--}950\text{ cm}^{-1}$: the CO stretching region; $950\text{--}700\text{ cm}^{-1}$: the side-groups deformational-region (COH,

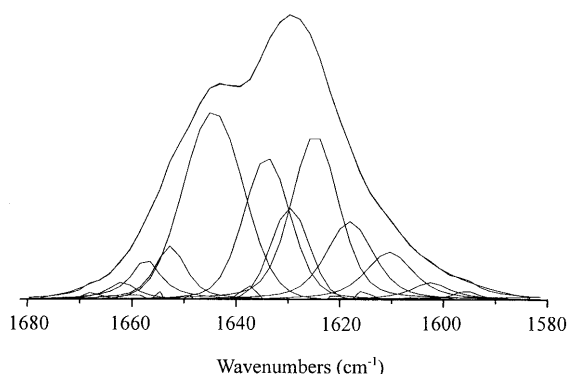


Fig. 4. The curve-fit result for Nd-galactitol.

Table 4

The C–O, C–C distance and the angles of galactitol and its metal complexes

	Galactitol ³⁶	Pr-galactitol ²⁷	Nd-galactitol
<i>Distance (Å)</i>			
C-1–O-1	1.438, 1.421	1.443	1.440
C-2–O-2	1.428, 1.436	1.442	1.443
C-3–O-3	1.437, 1.435	1.432	1.438
C-1–C-2	1.523, 1.528	1.518	1.510
C-2–C-3	1.513, 1.507	1.522	1.515
C-1–C-1a	1.531	1.535	1.533
<i>Angles (°)</i>			
C-1–C-2–C-3	111.8, 112.1	114.7	115.0
C-2–C-1–C-1a	113.1	112.2	113.0
O-3–C-3–C-2	110.1, 109.6	108.8	108.8
C-3–C-2–O-2	110.3, 110.3	108.9	108.8
O-2–C-2–C-1	109.1, 108.4	105.7	105.3
C-2–C-1–O-1	110.7	106.9	107.3
O-1–C-1–C-1a	109.1	108.2	107.9

CCH, OCH), which includes the important fingerprint or anomeric bands between 930 and 840 cm^{-1} , and an appreciable contribution from the stretching of C–C; and $700\text{--}500\text{ cm}^{-1}$: exocyclic deformations (CCO, CCC, COH).³⁷ Each peak is coupled by many vibration modes. In comparison with the spectrum of galactitol, the peak positions and relative intensities of the peaks are changed in the spectra of the metal complexes. Because the coordination modes of Pr and Nd are the same, the spectra in this region are similar. There are five evident peaks: $1099, 1067, 1026, 978, 951\text{ cm}^{-1}$ for the Nd-complex and $1099, 1067, 1026, 977, 950\text{ cm}^{-1}$ for the Pr-complex, corresponding to $1118, 1104, 1079, 1049, 1031, 1001\text{ cm}^{-1}$ in the spectrum of galactitol. The IR spectra show excellent agreement with corresponding crystal structures. For example, the 1001 cm^{-1} peak could be assigned to 17C-2-C-3 , 12O-3-C-3-H , 6C-2-C-3-O-3 , 6C-2-O-2 and 5C-3-O-3-H .³⁸ After formation of the complexes, the C-2–C-3, C-2–O-2 (mainly contributors to PED) distances become longer (Table 4), the force constants $K_{\text{C-2-C-3}}$ and $K_{\text{C-2-O-2}}$ are decreased and the peak is shifted to a lower wavenumber: 977 cm^{-1} (Pr-complex) or 978 cm^{-1} (Nd-complex). The change in peak positions and relative intensities in the IR spectra are consistent with the variation in bond distances and angles determined from the crystal structures.

In conclusion, the IR results reflect minor differences in the structures and is a useful technique to evaluate metal–sugar complex formation.

3. Experimental

Materials.— NdCl_3 , PrCl_3 were prepared and crystallized from the corresponding rare earth oxides of high purity (99.99%). Galactitol (AR) was used as supplied.

Preparation of galactitol complexes.—Galactitol (3 mmol) and 2 equiv of the metal chlorides were dissolved in H_2O –EtOH and heated to make concd solns. The flasks were then sealed until the complexes crystallized. Anal. Calcd for $2\text{PrCl}_3 \cdot \text{C}_6\text{H}_{14}\text{O}_6 \cdot 14\text{H}_2\text{O}$: C, 7.758; H, 4.557. Found: C, 7.942; H, 4.399.

Anal. Calcd for $2\text{NdCl}_3 \cdot \text{C}_6\text{H}_{14}\text{O}_6 \cdot 14\text{H}_2\text{O}$: C, 7.703; H, 4.525. Found: C, 8.007; H, 4.311.

Physical measurements.—The structure of $2\text{NdCl}_3 \cdot \text{C}_6\text{H}_{14}\text{O}_6 \cdot 14\text{H}_2\text{O}$ was determined on a Rigaku AF6S diffractometer using monochromatic Mo K_α radiation ($\lambda = 0.71073 \text{ \AA}$) in the θ range from 2.24 to 25° at 293(2) K. The final cycle of full-matrix least-square refinement was based on 2731 observed reflections. Calculations were completed with the SHELX-97 program. The IR spectra of $2\text{NdCl}_3 \cdot \text{C}_6\text{H}_{14}\text{O}_6 \cdot 14\text{H}_2\text{O}$ and $2\text{PrCl}_3 \cdot \text{C}_6\text{H}_{14}\text{O}_6 \cdot 14\text{H}_2\text{O}$ ($4000\text{--}650 \text{ cm}^{-1}$) were recorded on a Nicolet Magna-IR 750 spectrometer, 128 scans at 4 cm^{-1} resolution.

Acknowledgements

The authors thank the National Natural Science Foundation of China for the grants (nos. 29671002 and 39730160) and the State Key Project for Fundamental Research of MOST (G1998061311) to support this work, and are grateful to Dr Yizhuang Xu, Miss Xu Zhang and Hui Liu of the Department of Chemistry, Peking University, Beijing, China, for their help.

References

1. Sauchelli, V. *Trace Elements in Agriculture*; Van Nostrand: New York, 1969; p. 248.
2. Holm, R. P.; Berg, J. M. *Pure Appl. Chem.* **1984**, *56*, 1645–1657.
3. Predki, P. F.; Whitfield, D. M.; Sarkar, B. *Biochem. J.* **1992**, *281*, 835–841.
4. Templeton, D. M.; Sarkar, B. *Biochem. J.* **1985**, *230*, 35–42.
5. Weis, W. I.; Drickamer, K.; Hendrickson, W. A. *Nature* **1992**, *360*, 127–134.
6. Drickamer, K. *Nature* **1992**, *360*, 183–186.
7. Rendleman Jr., J. A. *Adv. Carbohydr. Chem.* **1966**, *21*, 209–271.
8. Angyal, S. J. *Adv. Carbohydr. Chem. Biochem.* **1989**, *47*, 1–43.
9. Alekseev, Yu. E.; Garnovskii, A. D.; Zhdanov, Yu. A. *Usp. Khim.* **1998**, *67*, 723–744.
10. Burger, K.; Nagy, L. *Biocoordination Chemistry: Coordination Equilibria in Biologically Active Systems*; 1990; pp. 236–283.
11. Jean-Francois, V.; Stella, C.; Feibo, X.; Debbie, C. *Progr. Inorg. Chem.* **1998**, *47*, 837–945.
12. Bandwar, R. P.; Rao, C. P. *Curr. Sci.* **1997**, *72*, 788–796.
13. Sigel, H. *Chem. Soc. Rev.* **1993**, *22*, 255–267.
14. Whitfield, D. M.; Stojkovski, S.; Sarkar, B. *Coord. Chem. Rev.* **1993**, *122*, 171–225.
15. Yano, S.; Otsuka, M. In *Metal Ions in Biological Systems*; Sigel, H., Ed. 1996; Vol. 32, pp. 27–60.
16. Piarulli, U.; Floriani, C. *Progr. Inorg. Chem.* **1997**, *46*, 393–429.
17. Gyurcsik, B.; Nagy, L. *Coord. Chem. Rev.* **2000**, *203*, 81–148.
18. Yano, S. *Coord. Chem. Rev.* **1988**, *92*, 113–156.
19. Junicke, H.; Bruhn, C.; Kluge, R.; Serianni, A. S.; Steinborn, D. J. *Am. Chem. Soc.* **1999**, *121*, 6232–6241.
20. Cook, W. J.; Bugg, C. E. In *Metal–Ligand Interactions in Organic Chemistry and Biochemistry*; Pullman, B.; Goldblum, W., Eds.; 1977; Vol. 2, pp. 231–256.
21. Wang, K. S. *Afr. J. Chem.* **1997**, *50*, 232.
22. Gao, X. X. *The Application of Rare Earths in Agriculture and Electroanalysis Chemistry*; Peking University Press: Beijing, 1997.
23. Song, Y. Y.; Xu, Y. Z.; Weng, S. F.; Wang, L. B.; Li, X. F.; Zhang, T. F.; Wu, J. G. *Biospectroscopy* **1999**, *5*, 371–377.
24. Xie, D. T.; Wang, L. B.; Wu, J. G.; Xu, G. X. *J. Rare Earths* **1999**, *17*, 81–82.
25. Ni, J. Z. *Bioinorganic Chemistry of Lanthanides*; Science Press: Beijing, 1995.
26. Israëli, Y.; Morel, J.-P.; Morel-Desrosiers, N. *Carbohydr. Res.* **1994**, *263*, 25–33.
27. Angyal, S. J.; Craig, D. C. *Carbohydr. Res.* **1993**, *241*, 1–8.
28. Lohmar Jr., R. L. In *The Carbohydrates*; Pigman, W., Ed.; Academic Press: New York, 1957; p. 241.
29. Kinoshita, J. H.; Merola, L. O.; Dikmak, E. *Exp. Eye Res.* **1962**, *1*, 405.
30. Zhao, Y.; et al. *J. Mol. Struct.* (accepted).
31. Yang, Y. M.; Weng, S. F.; Wu, J. G.; Xu, G. X. *Chem. J. Chin. Univ.* **1994**, *15*, 646–650.
32. Hong, L.; Guo, H.; Xu, D. F.; Wu, J. G. *Microchim. Acta* **1988**, *1*, 215–217.
33. Yang, L. Q.; Wu, J. G.; Zhou, Q.; Bian, J.; Yang, Y. M.; Xu, D. F.; Xu, G. X. *Microchim. Acta* **1997**, *14*, 251–252.
34. Wu, J. G. *Modern Fourier Transform Spectroscopy Techniques and its Applications*; Science and Technology References Press: Beijing, 1994.
35. Tian, W.; Yang, L. M.; Xu, Y. Z.; Weng, S. F.; Wu, J. G. *Carbohydr. Res.* **2000**, *324*, 45–52.
36. Berman, H. M.; Rosentein, R. D. *Acta Crystallogr., Sect. B* **1968**, *24*, 441–534.
37. Mathlouthi, M.; Koenig, J. L. *Adv. Carbohydr. Chem. Biochem.* **1986**, *44*, 7–89.
38. Zhbakov, R. G.; Andrianov, V. M.; Ratajczak, H.; Marchewka, M. *Zh. Strukt. Khim.* **1995**, *36*, 430–442.